Mechanical properties and electrical conductivity of TiN–Al$_2$O$_3$ nanocomposites

Jingguo Li, Lian Gao*, Jingkun Guo

State Key Lab of High Performance Ceramics and Superfine Microstructure, Shanghai Institute of Ceramics, Chinese Academy of Sciences, Shanghai 200050, People's Republic of China

Abstract

TiN–Al$_2$O$_3$ nanocomposites with various additions of TiN were prepared by hot pressing of nano TiN–Al$_2$O$_3$ powder that was produced by in-situ nitridation of nano TiO$_2$–Al$_2$O$_3$ powder. TiO$_2$–Al$_2$O$_3$ powder mixtures are prepared by a heterogeneous precipitation method. The effects of nano TiN particles on the mechanical properties and electrical conductivity of TiN–Al$_2$O$_3$ nanocomposites were studied. Experimental results show that the addition of 20 vol.% TiN could increase the bending strength of hot-pressed Al$_2$O$_3$ from 370 to 725 MPa and the fracture toughness from 3.40 to 5.27 MPa m$^{1/2}$, respectively. The resistivity of nanocomposites decreases with increasing amount of TiN and reaches to a minimum value of 5.5×10^{-3} Ω cm for the nanocomposite with 25 vol.% TiN. © 2002 Elsevier Science Ltd. All rights reserved.

Keywords: Electrical conductivity; Mechanical properties; Nanocomposites; TiN–Al$_2$O$_3$

1. Introduction

Alumina (Al$_2$O$_3$) ceramics are essential structural materials, but lower mechanical properties limit their applications. Since Niihara reported that nanocomposites reinforced with the sub-micrometer or nanometer second phase show excellent mechanical properties,[1,2] Al$_2$O$_3$-based nanocomposites were widely studied.

Titanium nitride (TiN) has a high melting temperature (2950 °C), good electroconductivity and high resistance to corrosion and oxidation.[3,4] These attractive physical and chemical properties suggest potentialities of TiN as a high-temperature material. Since the addition of TiN to the matrix material was reported to increase some mechanical properties, and to lower the electrical resistivity of the ceramic composites, the properties of TiN particles reinforced alumina or silicon nitride composites were widely studied.[5–7] Electroconductive Al$_2$O$_3$-based composites could be shaped by electrical discharge machining to manufacture complex components.[8–10] The good electroconductivity of the composites also results in their use as heating elements, igniters and heat exchangers. Moreover, they could be found many applications as wear-resistant materials and cutting tools.

The usual method used to prepare these ceramic composites is to add TiN particles directly into the matrix by ball milling. Such materials exhibit poor characteristics, which result from an inadequate dispersion process and the lack of sinterability caused by the large volume fraction of inert dispersion required for the electroconductivity. The mechanical properties and the electroconductivity of ceramic materials are strongly affected by the distribution of the electroconductive TiN second phase. Thus, it is necessary to improve the processing route to prepare materials with a better distribution of components. A preferable alternative is the in-situ formation of the second phase to obtain optimum properties.

In the present work, we described a novel method to prepare TiN–Al$_2$O$_3$ nanocomposites by in-situ formation of the TiN second phase. Dense TiN–Al$_2$O$_3$ nanocomposites with 5–25 vol.% TiN were sintered by hot pressing of nano TiN–Al$_2$O$_3$ powders. The mechanical properties and electrical conductivity of the sintered bodies were evaluated.

2. Experimental

The flow chart for preparation of TiN–Al$_2$O$_3$ nanocomposite powder is shown in Fig. 1. The α-Al$_2$O$_3$ and tetra-butyl titanate were mixed in calculated propor-

tions and homogenized by ball milling using anhydrous ethanol as the liquid medium for 8 h. Distilled water was dripped into the vigorously-stirred mixed solution of α-Al_2O_3 and tetra-butyl titanate. The tetra-butyl titanate was hydrolyzed to form nano TiO_2 particles on the surface of α-Al_2O_3 powder. After separation from the mother solution, precipitates were washed by distilled water and finally by anhydrous ethanol. After the final filtration, the cake was dried at 120 °C and subsequently calcined at 450 °C for 2 h to obtain nano TiO_2–α-Al_2O_3 composite powder. Nano TiN–Al_2O_3 powders were prepared by in-situ direct nitridation of nano TiO_2–α-Al_2O_3 powders with NH_3 as reducing agent in a tube furnace. TiN–Al_2O_3 nanocomposite powders with 5–25 vol.% TiN were sintered by hot-pressing at temperatures between 1400 and 1650 °C and a pressure of 30 MPa for 60 min under N_2 atmosphere.

The density of the sintered samples was measured using the Archimedes method. The theoretical density value of the samples was calculated according to the rule of mixtures using 3.98 g cm^{-3} for Al_2O_3 and 5.44 g cm^{-3} for TiN, assuming that no chemical reactions take place between the matrix material Al_2O_3 and the second phase TiN. For mechanical testing, the hot pressed samples were cut and ground into rectangular bar specimens (4×3×35 mm). The bending strength was measured with Instron-1195 using the three point bending test with a span length of 30 mm and crosshead speed of 0.5 mm/min. Measurements of the hardness and the fracture toughness were conducted with Akashi(AVK-

A) by indentation using a pyramidal indenter and applying a 10 kg load for 10 s. The resistivity of sintered bodies was measured by the four-probe method.

The morphology of the TiN–Al_2O_3 nanocomposite powder was observed using TEM (Jeol-2010CX). The microstructure of sintered bodies was observed using SEM (LX-30 ESEM, Philips). The phase compositions of the TiN–Al_2O_3 nanocomposite powders and sintered bodies were identified by XRD (Rigaku D/MAX rB).

3. Results and discussion

3.1. TEM observation and XRD identification of TiN–Al₂O₃ nanocomposite powder

TEM micrograph of the TiN–Al_2O_3 nanocomposite powder prepared by in-situ direct nitridation is shown in Fig. 2. It can be observed that TiN nanoparticles with an average diameter around 40–50 nm are homogeneously deposited on the surface of Al_2O_3 particles. This indicates that in-situ formation of TiN second phase results in a better distribution of components. Fig. 3 is an XRD pattern of TiN–α-Al_2O_3 nanocompo-
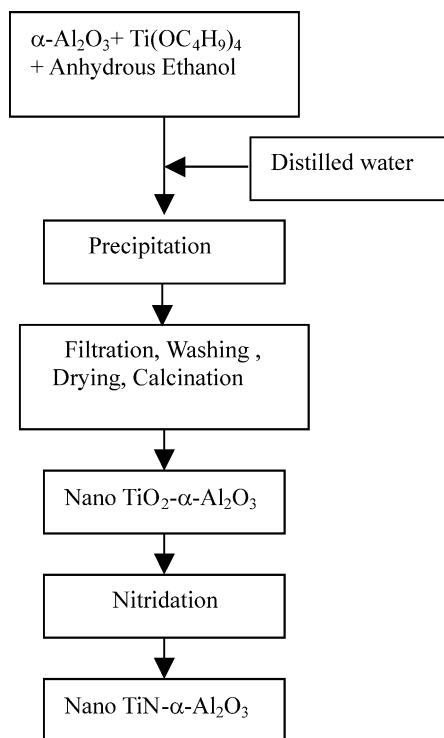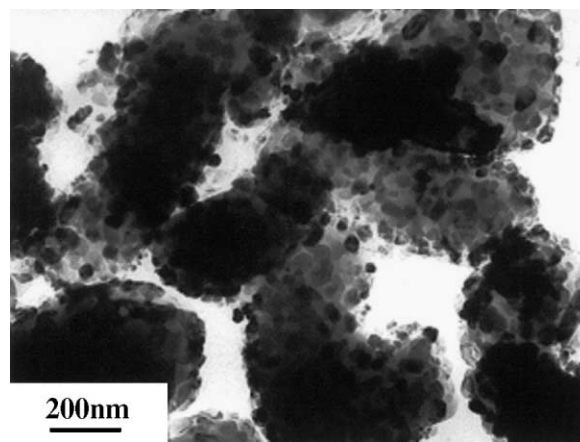

200nm

Fig. 2. TEM micrograph of nano TiN–Al_2O_3 powder.
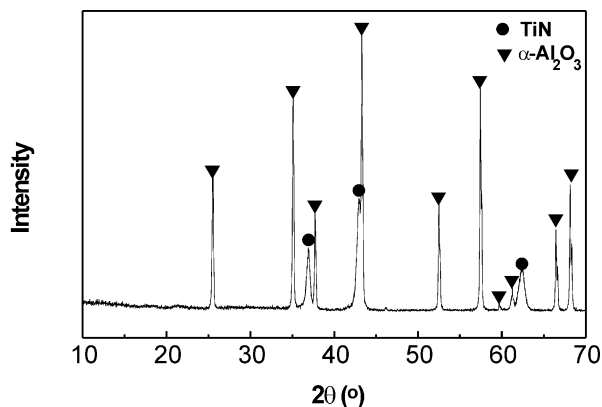
Fig. 3. XRD pattern of nano TiN–Al_2O_3 powder prepared by in-situ direct nitridation at 900 °C for 5 h.

Fig. 1. Flow chart for preparation of nano TiN–α-Al_2O_3 powder.

site powder prepared by in-situ direct nitridation at 900 °C for 5 h. Only TiN and α-Al_2O_3 phase could be detected, as shown in Fig. 3. It suggests that the TiO_2 nanoparticles deposited on the surface of α-Al_2O_3 particles are completely converted to TiN after nitridation at 900 °C for 5 h.

3.2. Densification and XRD identification of sintered nanocomposites

The nanocomposite powder with 20 vol.% TiN was hot pressed at different temperatures, and the relative densities of the sintered bodies are shown in Fig. 4. It can be seen that the relative densities of all the samples hot-pressed between 1450 and 1650 °C are higher than 99% of theoretical density. Moreover, all the specimens hot-pressed at 1550 °C with the addition of 5–25 vol.% TiN has a relative density higher than 99%. This densification temperature is lower than that reported by others.[6] It suggests that TiN–Al_2O_3 nanocomposite powder prepared by in-situ direct nitridation has a good sinterability.

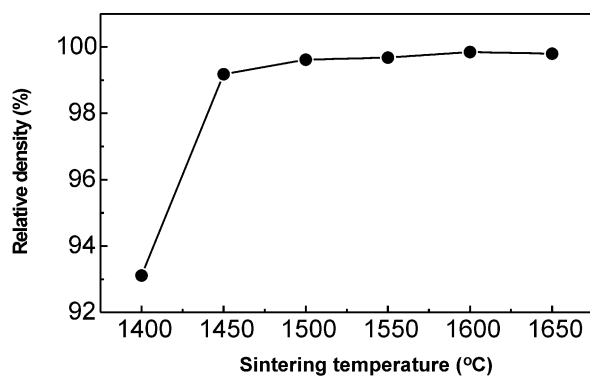Fig. 5 is an X-ray diffraction pattern of 20 vol.% TiN–Al_2O_3 nanocomposite sintered at 1550 °C for 60 min. XRD results reveal that the prepared nanocomposite is composed of TiN (cubic) and α-Al_2O_3. The result indicates that no chemical reaction occurs between the second phase and the matrix.

3.3. Morphology of polished surface and fracture cross-sections

Fig. 6 shows the back-scattered SEM micrograph of the polished surface of hot-pressed 20 vol.% TiN–Al_2O_3 nanocomposite. Black grains are Al_2O_3, while white particles located among Al_2O_3 grains are TiN. TiN grains were uniformly dispersed in Al_2O_3 matrix, as shown in Fig. 6. Fig. 7 shows the microstructure of the fracture cross-sections of TiN–Al_2O_3 nanocomposites with various TiN contents. It can be seen that the fracture morphology and grain size were significantly influenced by the TiN contents in these materials. The fracture mode of TiN–Al_2O_3 nanocomposites with 5 vol.% TiN and 10 vol.% TiN [Fig. 7(a) and (b)] was mainly intergranular. But, the fracture modes of TiN–Al_2O_3 nanocomposites with 15 vol.% TiN and 20 vol.% TiN [Fig. 7 (c) and (d)] were intergranular and transgranular. The explanation for fracture mode change was that the grain boundaries in TiN–Al_2O_3 nanocomposites were strengthened, inhibiting intergranular crack propagation.

3.4. Mechanical properties

Fig. 8 shows the Vickers hardness of TiN–Al_2O_3 nanocomposites sintered by hot pressing at 1550 versus TiN content. It can be seen that the Vickers hardness of TiN–Al_2O_3 nanocomposites reaches to a hardness of 19 GPa, which was almost the same for different TiN contents from 5 to 25 vol.% and no significant difference from that of pure Al_2O_3.

Fig. 9 shows the bending strength of TiN–Al_2O_3 nanocomposites sintered at 1550 versus TiN content. It can be seen that the bending strength of TiN–Al_2O_3

Fig. 4. Relative density of 20 vol.% TiN–Al_2O_3 nanocomposite versus sintering temperature.

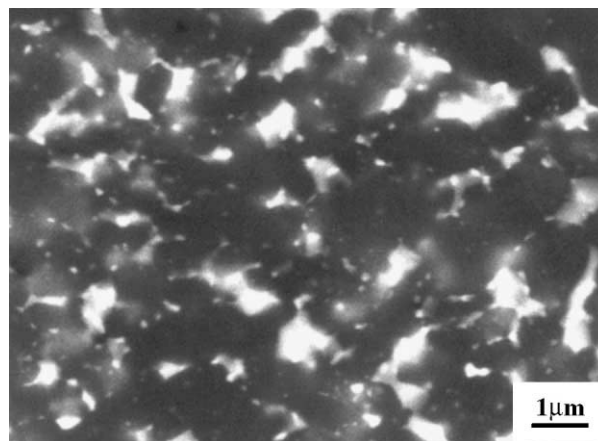Fig. 5. XRD pattern of 20 vol.% TiN–Al_2O_3 nanocomposite sintered by hot pressing at 1550 °C.

Fig. 6. Back-scattered SEM micrograph of polished surface of 20 vol.% TiN–Al_2O_3 nanocomposite.
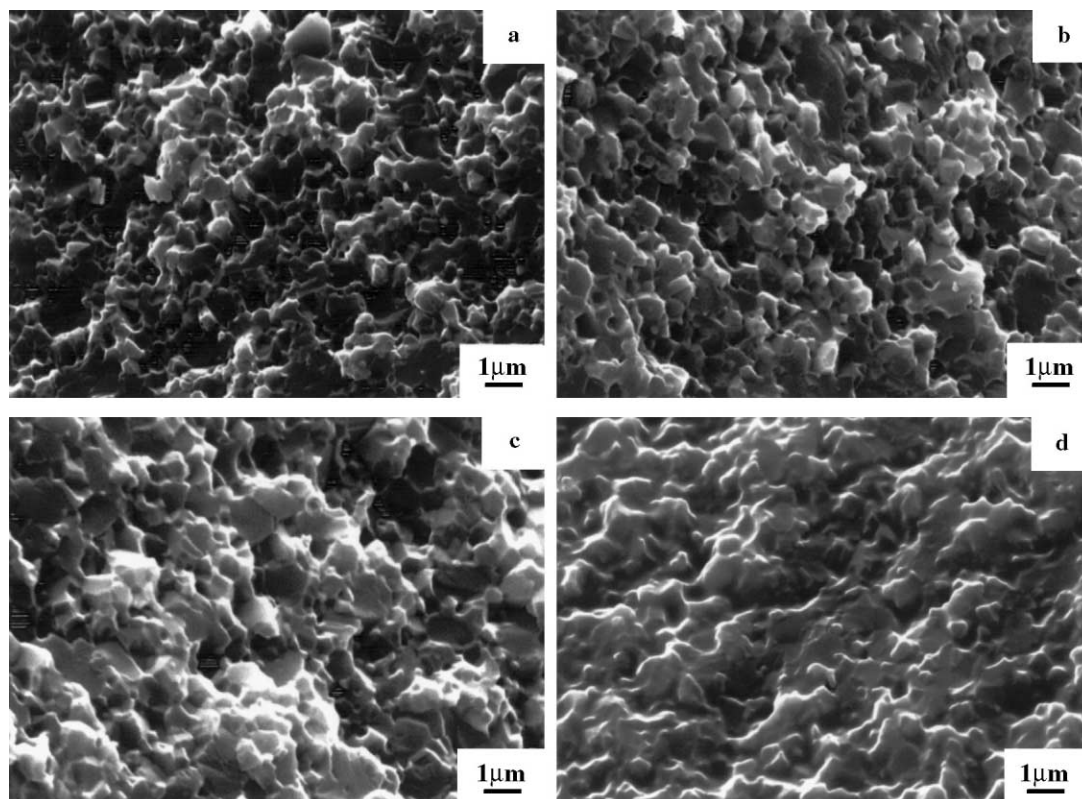
Fig. 7. SEM micrographs of fracture cross-sections of the nanocomposites: (a) 5 vol.% TiN–Al₂O₃; (b) 10 vol.% TiN–Al₂O₃; (c) 15 vol.% TiN–Al₂O₃; (d) 20 vol.% TiN–Al₂O₃.
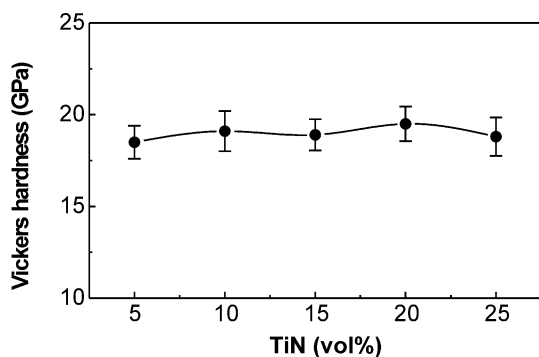

Fig. 8. Vickers hardness of TiN–Al₂O₃ nanocomposites sintered at 1550 °C versus TiN content.

nanocomposites with various TiN contents from 5 to 25 vol.% was higher than that of monolithic Al₂O₃ ceramics and the highest bending strength (725 MPa) was achieved at 20 vol.% TiN. This bending strength value is much higher than that of monolithic Al₂O₃ ceramics (370 MPa). Fig. 10 shows the bending strength of 20 vol.% TiN–Al₂O₃ nanocomposites versus sintering temperature. The bending strength of TiN–Al₂O₃ nanocomposites sintered at temperatures from 1500 to 1650 °C was higher than that of monolithic Al₂O₃ ceramics, but, the highest value was achieved at 1550 °C. The addition of TiN nanoparticles improves the microstructure and strengthens grain boundaries, which lead

to increase in the bending strength of the TiN–Al₂O₃ nanocomposites.

Fig. 11 shows the fracture toughness of TiN–Al₂O₃ nanocomposites sintered by hot pressing at 1550 °C versus TiN content. The fracture toughness of all the composites is higher than that of Al₂O₃ matrix, while the highest value of 5.27 Mpa m$^{1/2}$ is achieved at 15 vol.% TiN, as shown in Fig. 11. For particulate reinforced composites, many toughening mechanisms such as crack pinning, the microcrack toughening, crack deflection, residual stress toughening and crack bridging have been proposed. Since some of these toughening mechanisms were often active at the same time, it is difficult to indicate a prevailing toughening mechanism. For TiN–Al₂O₃ composites, residual stress and microcrack toughening can be excluded due to the very similar value of the thermal expansion coefficients of both constituent phases[6] and possible toughening mechanisms are crack deflections and/ or crack pinning.

3.5. Electrical conductivity

The mechanism of electrical conduction for TiN–Al₂O₃ composite materials is the formation of a network of TiN electrical conductive phase within the Al₂O₃ matrix, so that the distribution of TiN particles is one of the most important factors for the electro-
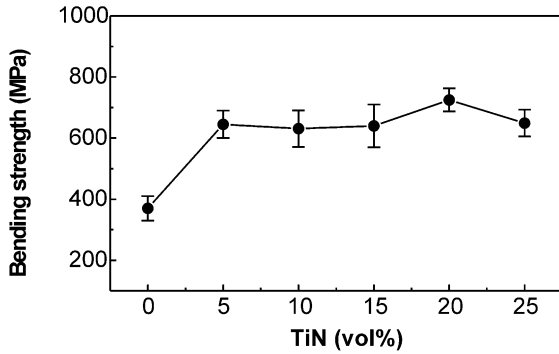
Fig. 9. Bending strength of TiN–Al$_2$O$_3$ nanocomposites sintered at 1550 °C versus TiN content.
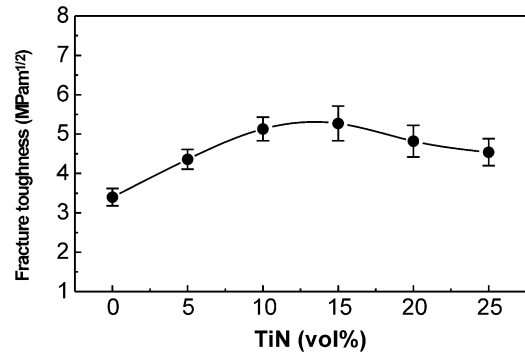

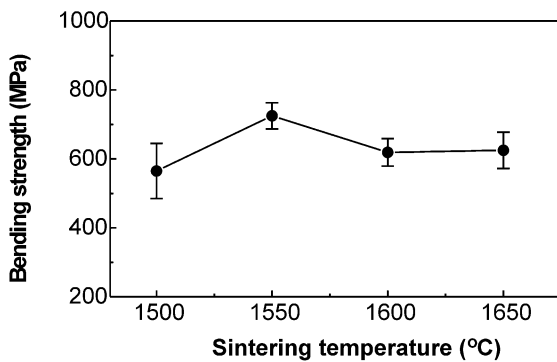Fig. 11. Fracture toughness of TiN–Al$_2$O$_3$ nanocomposites sintered at 1550 °C versus TiN content.

Fig. 10. Bending strength of 20 vol.% TiN–Al$_2$O$_3$ nanocomposites versus sintering temperature.
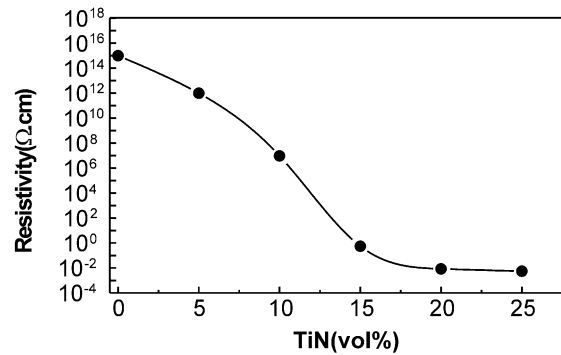

Fig. 12. Resistivity of TiN–Al$_2$O$_3$ nanocomposites sintered at 1550 °C versus TiN content.

conductivity.[11] From the back-scattered SEM micrograph of 20 vol.% TiN–Al$_2$O$_3$ nanocomposites shown in Fig. 6, it can be observed that TiN particles were homogeneously dispersed in the matrix. Therefore, the nanocomposites prepared by in-situ formation of TiN second phase were expected to have a high electroconductivity, and our resistivity measurements were performed to confirm it.

Fig. 12 shows the relationship between the TiN content and the resistivity of nanocomposites sintered at 1550 °C with a pressure of 30 MPa for 60 min. The resistivity of nanocomposites decreases with increasing amount of TiN phase and reaches to a minimum value of 5.5×10^{-3} Ω cm for the nanocomposite with 25 vol.% TiN. The experimental results show that prepared TiN–Al$_2$O$_3$ nanocomposites have good electroconductivities, especially at low additions of TiN. The percolation concentration of nanocomposite is about 15 vol.% TiN. This value is lower than that reported for the microcomposites prepared by conventional methods.[5]

4. Conclusions

Dense TiN–Al$_2$O$_3$ nanocomposites with high bending strength, high fracture toughness and good electrical conductivity were successfully prepared by using a novel method.

Experimental results indicate that TiN–Al$_2$O$_3$ nanocomposite powder prepared by in-situ direct nitridation of nano TiO$_2$–Al$_2$O$_3$ powder could be sintered to dense at a relatively low temperature by the hot pressing method. The bending strength and the fracture toughness of prepared nanocomposites have been greatly improved and the hardness is almost identical to that of Al$_2$O$_3$ matrix. The prepared nanocomposites have lower percolation concentration and high electroconductivity. The experimental results suggest that the present method is effective for improving the mechanical properties and electrical properties of TiN–Al$_2$O$_3$ nanocomposites.

References

1. Niihara, K., New design concept of structural ceramics-ceramics nanocomposites. *J. Ceram. Soc. Jpn*, 1991, **99**, 974–982.
2. Niihara, K., Nakahiara, A. and Sekino, T., New nanocomposite structural ceramics. In *MRS Symposium Proceedings*, Vol. 286, ed. S. Lomareneni, J. C. Parker and G. J. Thommas. Boston, 1992, pp. 405–412.
3. Mukerji, J. and Biswas, S. K., Synthesis, properties and oxidation of alumina-titanium nitride composites. *J. Am. Ceram. Soc.*, 1990, **73**, 142–145.

4. Gogotsi, Y. G. and Porz, F., Mechanical properties and oxidation behaviour of Al_2O_3-TiN composites. *J. Am. Ceram. Soc.*, 1992, **78**, 2251–2259.

5. Rak, Z. S. and Czechowski, J., Manufacture and properties of Al_2O_3-TiN particulate composites. *J. Eur. Ceram. Soc.*, 1998, **18**, 373–380.

6. Bellosi, A., Portu, G. D. and Guicciardi, S., Preparation and properties of electroconductive Al_2O_3-based composites. *J. Eur. Ceram. Soc.*, 1992, **10**, 307–315.

7. Bellosi, A., Guicciardi, S. and Tampieri, A., Development and characterization of electroconductive Si_3N_4-TiN composites. *J. Eur. Ceram. Soc.*, 1992, **9**, 83–93.

8. Tsugeki, K., Kato, T., Koyanagi, Y., Kusakabe, K. and Morooka, K., Electroconductivity of sintered bodies of α-Al_2O_3-TiN composite prepared by CVD reaction in a fluidized bed. *J. Mater. Sci.*, 1993, **28**, 3168–3172.

9. Ramulu, M., EDM sinker cutting of ceramic particulate composite, SiC-TiB_2. *Adv. Ceram. Mater.*, 1998, **3**, 324–327.

10. Petrotes, N. F. and Gadalla, A. M., Electrical discharge machining of advanced ceramics. *Am. Ceram. Soc. Bull.*, 1998, **67**, 1048–1052.

11. Lux, F., Models proposed to explain the electrical conductivity of mixtures made of conductive and insulating materials. *J. Mater. Sci.*, 1993, **28**, 285–301.